



UNIVERSITI PUTRA MALAYSIA

**CHARACTERISATION OF ANTIMONY AND ANTIMONY-BISMUTH
OXIDES SYNTHESISED BY PRECIPITATION TECHNIQUE**

NORHAYATI BT MOHD NOOR

FS 2007 47



**CHARACTERISATION OF ANTIMONY AND ANTIMONY-BISMUTH
OXIDES SYNTHESISED BY PRECIPITATION TECHNIQUE**

By

NORHAYATI BT MOHD NOOR

**Thesis Submitted to the School of Graduate Studies, Universiti Putra Malaysia, in
Fulfilment of the Requirements for the Degree of Master of Science**

April 2007



TABLE OF CONTENTS

	Page
DEDICATION	ii
ABSTRACT	iii
ABSTRAK	v
ACKNOWLEDGEMENTS	vii
APPROVAL	viii
DECLARATION	x
LIST OF TABLES	xiii
LIST OF FIGURES	xv
LIST OF ABBREVIATIONS	xviii
CHAPTER	
1 GENERAL INTRODUCTION	
1.1 Antimony Oxide	1
1.2 Preparation of Antimony Oxide	6
1.2.1 Preparation Methods	6
1.2.2 Effects of Preparation Parameters	9
1.3 Industrial Application of Antimony Oxide	14
1.3.1 The Role of Antimony Oxide as a Mixed Oxide Catalysts	15
1.4 Bismuth Oxide	20
1.5 Objectives of the Study	22
2 METHODOLOGY	
2.1 Materials and Gases	23
2.2 Preparation of Antimony Oxide via Different Preparation Parameters	24
2.2.1 Starting Material, Precipitation Route, Precipitating Agent and pH	24
2.3 Preparation of Antimony-Bismuth Oxide via Coprecipitation Method	26
2.4 Characterizations	27
2.4.1 Differential Thermogravimetry/Thermogravimetric Analysis (DTG/TGA)	27
2.4.2 Powder X-ray Diffraction (XRD)	27
2.4.3 Fourier Transform Infrared (FT-IR) Spectroscopy	28
2.4.4 BET Surface Area Measurements	28
2.4.5 Scanning Electron Microscopy (SEM)	29
2.4.6 Temperature-Programmed Reduction (TPR) in H ₂	29



3	RESULTS AND DISCUSSION	30
3.1	Effect of Precipitation Route on Antimony Oxide Properties	30
3.1.1	Titration Curve and Yield of Antimony Oxide	30
3.1.2	Differential Thermogravimetry/Thermogravimetric Analysis (DTG/TGA)	34
3.1.3	Phase Identification using Powder XRD Technique	37
3.1.4	Fourier Transform Infrared (FT-IR) Spectroscopy	41
3.1.5	BET Surface Area Measurements	43
3.1.6	Scanning Electron Microscopy (SEM)	45
3.1.7	Conclusion	47
3.2	Effect of Precipitating Agent Concentration on Antimony Oxide Properties	48
3.2.1	Effect of Precipitating Agent Concentration: NaOH as a Precipitating Agent	48
3.2.2	Effect of Precipitating Agent Concentration: NH ₄ OH as a Precipitating Agent	61
3.3	Effect of pH by using NaOH Solution as a Precipitating Agent and Antimony(III) Acetate as a Salt Solution	75
3.3.1	Titration Curve and Yield of Antimony Oxide	76
3.3.2	Phase Identification using Powder XRD Technique	78
3.3.3	Fourier Transform Infrared (FT-IR) Spectroscopy	81
3.3.4	BET Surface Area Measurements	81
3.3.5	Scanning Electron Microscopy (SEM)	83
3.3.6	Conclusion	86
3.4	Preparation of Antimony-Bismuth Oxides	87
3.4.1	Titration Curve and Yield of Antimony-Bismuth Oxide	87
3.4.2	Thermogravimetric Analysis (TGA)	90
3.4.3	Phase Identification using Powder XRD Technique	92
3.4.4	Fourier Transform Infrared (FT-IR) Spectroscopy	95
3.4.5	BET Surface Area Measurements	97
3.4.6	Scanning Electron Microscopy (SEM)	98
3.4.7	Temperature-Programmed Reduction (TPR) in H ₂	100
3.4.8	Conclusion	102
4	SUMMARY AND CONCLUDING REMARKS	104
	REFERENCES	106
	APPENDICES	115
	BIODATA OF THE AUTHOR	118



Special Dedication To

My Beloved Husband & Daughter

*Khairul Affendy Ismail
Nur Afiqah Irdina*

My Dearest Ma & Abah

*Hasnah Ismail
Mohd Noor Salleh*

My Dear Brothers & Sisters

*Mohd Hilmi
Mohd Izani
Mohd Nabil
Mohd Hanif Ezzat
Norsyafiqah
Nor Aliya Auni*

My Dear Parents-in-law

*Ismail Abd. Rahman
Shaiyah Hamat*

Thanks to their love and support for all the time no matter what had happened.

“... Alhamdulillah”



Abstract of thesis presented to the Senate of Universiti Putra Malaysia in fulfillment of the requirement for the degree of Master of Science

**CHARACTERISATION OF ANTIMONY AND ANTIMONY-BISMUTH
OXIDES SYNTHESISED BY PRECIPITATION TECHNIQUE**

By

NORHAYATI BINTI MOHD NOOR

April 2007

Chairman : Associate Professor Dr. Abdul Halim Abdullah, PhD

Faculty : Science

Antimony oxide exists in several different phases and this single oxide has generated considerable interest in applications such as polyethylene terephthalate (PET) production and semiconductor devices manufacturing. In this study, antimony oxide and antimony bismuth oxide have been prepared via precipitation and coprecipitation technique, respectively. The influence of various preparation parameters (starting material, precipitating agent, precipitation route and pH) on the prepared antimony oxide has been investigated. The characteristics of the samples (antimony oxide and antimony bismuth oxide) were determined by Differential Thermogravimetry/Thermogravimetric Analysis (DTG/TGA), Powder X-ray Diffraction Analysis (XRD), Fourier Transform Infrared Analysis (FTIR), Brunauer-Emmett-Teller Surface Area Measurements (BET) and Scanning Electron Microscopy (SEM). Extent of reduction of antimony bismuth oxide



was investigated by employing Temperature-Programmed Reduction in H_2 (TPR) technique.

Starting material and precipitation route have influenced the formation of the final products which have given the different surface area. By using antimony(III) acetate (raw material) via forward precipitation route, a single phase of Sb_2O_3 senarmontite phase with high surface area can be obtained. As the concentration of precipitating agent, NaOH is increased, the formation of antimony oxide phase changed from single phase to mixed phase which was vice versa with increasing of NH_4OH concentration. The sample of high surface area with corresponding ultrafine particle could be achieved at optimum condition (0.6 M of NaOH concentration).

The microstructural change of prepared antimony oxide was determined at various pH values. The pH change does not effect the formation of antimony oxides phases but led to the higher surface area as the pH increases. The evolvement of the antimony bismuth oxide phase occurred as the NH_4OH concentration increases. The high surface area sample with small grain size can be obtained using 0.6 M NH_4OH . This sample gave small amount of oxygen removal in accordance to TPR result.

Abstrak tesis yang dikemukakan kepada Senat Universiti Putra Malaysia sebagai memenuhi keperluan untuk ijazah Master Sains

**PENCIRIAN ANTIMONI DAN ANTIMONI-BISMUT OKSIDA YANG
DISINTESIS MENGGUNAKAN TEKNIK PEMENDAKAN**

Oleh

NORHAYATI BINTI MOHD NOOR

April 2007

Pengerusi : Professor Madya Dr. Abdul Halim Abdullah, PhD

Fakulti : Sains

Antimoni oksida wujud di dalam beberapa fasa yang berlainan dan oksida tunggal ini telah mendapat perhatian di dalam pengaplikasian seperti penghasilan polietilena tereftalat (PET) dan pembuatan peranti semikonduktor. Di dalam kajian ini, antimoni oksida dan antimoni bismut oksida telah disediakan melalui teknik pemendakan dan kopemendakan. Kesan pelbagai parameter penyediaan (bahan pemula, agen pemendakan, arah pemendakan dan pH) ke atas antimoni oksida yang disediakan telah dikaji. Ciri-ciri bagi sampel antimoni oksida dan antimoni bismut oksida telah ditentukan dengan menggunakan Analisis Termogravimetri (DTG/TGA), Analisis Pembelauan X-ray (XRD), Analisis Spektroskopi Sinarmerah (FTIR), Pengukuran Luas Permukaan dengan kaedah BET dan Mikroskopi Pengimbas Elektron (SEM). Penurunan antimoni bismut oksida dikaji dengan menjalankan ujikaji Penurunan Berprogram Suhu (TPR).



Bahan pemula dan arah pemendakan telah mempengaruhi pembentukan hasil di mana ia telah memberikan luas permukaan yang berbeza. Dengan menggunakan antimoni triasetat sebagai bahan pemula melalui teknik pemendakan secara ke hadapan, fasa tunggal iaitu Sb_2O_3 fasa senarmontite yang mempunyai luas permukaan yang besar boleh dicapai. Bagi kajian kesan agen presipitasi; apabila kepekatan NaOH meningkat, pembentukan fasa antimoni oksida berubah daripada fasa tunggal kepada fasa campuran di mana keadaan sebaliknya berlaku apabila kepekatan NH_4OH ditingkatkan. Sampel dengan luas permukaan yang tinggi dan partikel yang halus boleh dicapai pada keadaan optimum (kepekatan NaOH adalah 0.6 M).

Perubahan struktur mikro pada antimoni oksida yang disediakan telah ditentukan pada pelbagai pH. Pembentukan fasa antimoni oksida tidak dipengaruhi oleh perubahan pH tetapi cenderung memberikan luas permukaan yang tinggi apabila pH ditingkatkan. Perkembangan fasa antimoni bismus oksida berlaku apabila kepekatan NH_4OH meningkat. Sampel yang mempunyai luas permukaan yang tinggi dan bersaiz butiran kecil boleh dihasilkan pada NH_4OH berkepekatan 0.6 M. Sampel ini memberikan amaun penyingkiran oksigen yang rendah berdasarkan keputusan TPR.

ACKNOWLEDGEMENTS

Bismillahirrahmanirrahim...

Glory and praise be to ALLAH s.w.t, the Almighty for providing me the strength and diligence to complete this dissertation despite several obstacles encountered throughout the progress of this study, which at time seemed insurmountable.

First of all, I would like to express my sincere and deepest gratitude to my supervisor Assoc. Professor Dr. Abdul Halim Abdullah for his guidance, understanding, concern and unlimited patience throughout the course of this work. I am also like to express my appreciation to my co-supervisors Assoc. Professor Dr. Irmawati Ramli and Assoc. Professor Dr. Mansur Hashim for their valuable guidance and advices.

Besides that, heartfelt thanks are extended to all the laboratory officers of the Chemistry Department, UPM especially to Mrs. Zaidina, Mrs. Rusnani and also to Mrs. Faridah from Institute of Bioscience for their kindness and willingness to help.

Special appreciation to all my good friends (Izan, Ernee, Yatod, Emy, Murni, Tim, Kak Sharmy, Hasbi, Raslan, Izham, Hairul, Asri, Saw, Hooi Hong and Chee Keong) for their companionship, joyfulness, support and encouragement.

Last but not least, thanks to all those who had contributed to the success of this work in one way or another especially my beloved husband, daughter, parents, sisters, brothers and parents-in-law for being supportive and understanding.

Financial support from University Putra Malaysia and the Ministry of Science, Technology and Innovation in the form of PASCA Graduate scheme is gratefully acknowledged.



I certify an Examination Committee met on 13th April 2007 to conduct the final examination of Norhayati Binti Mohd Noor on her Master of Science thesis entitled “Characterisation of Antimony and Antimony-Bismuth Oxides Synthesised by Precipitation Technique” in accordance with Universiti Pertanian Malaysia (Higher Degree) Act 1980 and Universiti Pertanian Malaysia (Higher Degree) regulations 1981. The Committee recommends that the student be awarded the degree of Master of Science.

Members of the Examination Committee were as follows:

Asmah Hj. Yahaya, PhD

Associate Professor
Faculty of Science
Universiti Putra Malaysia
(Chairman)

Anuar Kasim, PhD

Professor
Faculty of Science
Universiti Putra Malaysia
(Internal Examiner)

Zulkarnain Zainal, PhD

Professor
Faculty of Science
Universiti Putra Malaysia
(Internal Examiner)

Rosiyah Yahya, PhD

Associate Professor
Faculty of Science
Universiti Malaya
(External Examiner)

HASANAH MOHD. GHAZALI, PhD

Professor and Deputy Dean
School of Graduate Studies
Universiti Putra Malaysia

Date: 13 November 2007



This thesis submitted to the Senate of Universiti Putra Malaysia has been accepted as fulfillment of the requirements for the degree of Master of Science. The members of the Supervisory Committee are as follows:

Abdul Halim Abdullah, PhD

Associate Professor
Faculty of Science
Universiti Putra Malaysia
(Chairman)

Irmawati Ramli, PhD

Associate Professor
Faculty of Science
Universiti Putra Malaysia
(Member)

Mansor Hashim, PhD

Associate Professor
Faculty of Science
Universiti Putra Malaysia
(Member)

AINI IDERIS, PhD

Professor/ Dean
School of Graduate Studies
Universiti Putra Malaysia

Date:



DECLARATION

I hereby declare that the thesis is based on my original work except for the quotations and citations which have been duly acknowledged. I also declare that it has not been previously or concurrently submitted for any other degree at UPM or other institutions.

NORHAYATI BINTI MOHD NOOR

Date:



LIST OF TABLES

Table	Page
3.1 Percentage Yield of FSb, RSb, FKSb and RKSb samples before calcination	33
3.2 2θ and d values of uncalcined and calcined RKSb sample	40
3.3 Crystallite sizes of FSb, RSb, FKSb and RKSb samples	40
3.4 Grain sizes of FSb, RSb, FKSb and RKSb samples	44
3.5 Percentage yield of 01Sb, 02Sb, 04Sb, 06Sb, 08Sb and 10Sb samples before calcination	51
3.6 Crystallite sizes of (a) 01Sb, (b) 02Sb, (c) 04Sb, (d) 06Sb, (e) 08Sb and (f) 10Sb samples	52
3.7 Grain sizes of (a) 01Sb, (b) 02Sb, (c) 04Sb, (d) 06Sb, (e) 08Sb and (f) 10Sb samples	56
3.8 Percentage yield of 01SbN, 02SbN, 04SbN, 06SbN, 08SbN and 10SbN samples before calcination	63
3.9 Crystallite sizes of (a) 01SbN, (b) 02SbN, (c) 04SbN, (d) 06SbN, (e) 08SbN and (f) 10SbN samples	67
3.10 Grain sizes of (a) 01SbN, (b) 02SbN, (c) 04SbN, (d) 06SbN, (e) 08SbN and (f) 10SbN samples	70
3.11 Percentage yield of pH5Sb, pH9Sb and pH11Sb samples before calcination	78
3.12 Crystallite sizes of (a) pH5Sb, (b) pH9Sb and (c) pH11Sb samples	79



3.13	Grain sizes of (a) pH5Sb, (b) pH9Sb and (c) pH11Sb samples	83
3.14	Percentage yield of SB1, SB2 and SB3 samples before calcination	90
3.15	Crystallite sizes of (a) SB1, (b) SB2 and (c) SB3 samples	95
3.16	Grain sizes of (a) SB1, (b) SB2 and (c) SB3 samples	98
3.17	Total amount of oxygen atoms removed from SB2 sample	102



LIST OF FIGURES

Figure	Page	
1.1	Molecular structure of α -Sb ₂ O ₄ and β -Sb ₂ O ₄	4
3.1	Titration curves of (a) FKSb, (b) FSb, (c) RSb and (d) RKSb samples	31
3.2	Thermogram of (a) antimony(III) acetate, (b) antimony potassium tartarate and (c) prepared antimony oxides	34
3.3	Thermogram of uncalcined FSb sample	35
3.4	Thermogram of calcined (a) RKSb, (b) FKSb, (c) RSb and FSb samples	36
3.5	XRD patterns of calcined (a) FSb, (b) RSb, (c) FKSb and (d) RKSb samples	38
3.6	FTIR spectrums of calcined (a) FSb, (b) RSb, (c) FKSb and (d) RKSb samples	42
3.7	BET surface area measurement of calcined (a) FSb, (b) RSb, (c) FKSb and (d) RKSb samples	44
3.8	(a) SEM micrograph of FSb sample	45
	(b) SEM micrograph of RSb sample	46
	(c) SEM micrograph of FKSb sample	46
	(d) SEM micrograph of RKSb sample	47
3.9	Titration curves of (a) 01Sb, (b) 02Sb, (c) 04Sb, (d) 06Sb, (e) 08Sb and (f) 10Sb samples	49
3.10	XRD patterns of calcined (a) 01Sb, (b) 02Sb, (c) 04Sb, (d) 06Sb, (e) 08Sb and (f) 10Sb samples	53

3.11	FTIR spectrums of (a) 01Sb, (b) 02Sb, (c) 04Sb, (d) 06Sb, (e) 08Sb and (f) 10Sb samples	55
3.12	BET surface area measurement of calcined (a) 01Sb, (b) 02Sb, (c) 04Sb, (d) 06Sb, (e) 08Sb and (f) 10Sb samples	57
3.13	(a) SEM micrograph of 01Sb sample	58
	(b) SEM micrograph of 02Sb sample	59
	(c) SEM micrograph of 04Sb sample	59
	(d) SEM micrograph of 06Sb sample	60
	(e) SEM micrograph of 08Sb sample	60
	(f) SEM micrograph of 10Sb sample	61
3.14	Titration curves of (a) 01SbN, (b) 02SbN, (c) 04SbN, (d) 06SbN, (e) 08SbN and (f) 10SbN samples	62
3.15	XRD patterns of uncalcined (a) 01SbN, (b) 02SbN, (c) 04SbN, (d) 06SbN, (e) 08SbN and (f) 10SbN samples	65
3.16	XRD patterns of calcined (a) 01SbN, (b) 02SbN, (c) 04SbN, (d) 06SbN, (e) 08SbN and (f) 10SbN samples	66
3.17	FTIR spectrums of calcined (a) 01SbN, (b) 02SbN, (c) 04SbN, (d) 06SbN, (e) 08SbN and (f) 10SbN samples	69
3.18	BET surface area measurement of calcined (a) 01SbN, (b) 02SbN, (c) 04SbN, (d) 06SbN, (e) 08SbN and (f) 10SbN samples	71
3.19	(a) SEM micrograph of 01SbN sample	72
	(b) SEM micrograph of 02SbN sample	72
	(c) SEM micrograph of 04SbN sample	73
	(d) SEM micrograph of 06SbN sample	73



(e) SEM micrograph of 08SbN sample	74
(f) SEM micrograph of 10SbN sample	74
3.20 Titration curves of (a) pH5Sb, (b) pH9Sb and (c) pH11Sb samples	77
3.21 XRD patterns of calcined (a) pH5Sb, (b) pH9Sb and (c) pH11Sb samples	80
3.22 FTIR spectrums of calcined (a) pH5Sb, (b) pH9Sb and (c) pH11Sb samples	82
3.23 BET surface area measurement of calcined (a) pH5Sb, (b) pH9Sb and (c) pH11Sb samples	83
3.24 (a) SEM micrograph of pH5Sb sample	84
(b) SEM micrograph of pH9Sb sample	85
(c) SEM micrograph of pH11Sb sample	85
3.25 Titration curves of (a) SB1, (b) SB2 and (c) SB3 samples	88
3.26 Thermogram of uncalcined (a) SB1, (b) SB2 and (c) SB3 samples	91
3.27 XRD patterns of calcined (a) SB1, (b) SB2 and (c) SB3 samples	93
3.28 FTIR spectrums of calcined (a) SB1, (b) SB2 and (c) SB3 samples	96
3.29 BET surface area measurement of calcined (a) SB1, (b) SB2 and (c) SB3 samples	97
3.30 (a) SEM micrograph of SB1 sample	98
(b) SEM micrograph of SB2 sample	99
(c) SEM micrograph of SB3 sample	99
3.31 H ₂ -TPR spectra of SB2 sample	101

LIST OF ABBREVIATIONS

BET	Brunauer-Emmett-Teller
Bi	Bismuth
FTIR	Fourier Transform Infrared Spectroscopy
FWHM	Full-Width at Half Maximum
JCPDS	Joint Committee on Powder Diffraction Standards
PET	Polyethylene Terephthalate
SEM	Scanning Electron Microscopy
SOHIO	Standard Oil Company of Ohio
TGA	Thermogravimetric Analysis
TPR	Temperature Programmed Reduction
XRD	X-ray Diffraction



CHAPTER 1

GENERAL INTRODUCTION

1.1 Antimony Oxide

Antimony exists in the oxidation states of -3, 0, +3 and +5. There are a few phases in oxide of antimony which exist in several different compositions and display polymorphism. Sb_2O_3 , Sb_2O_4 , Sb_2O_5 and Sb_6O_{13} are the common phases of antimony oxide. Golunski *et al.* [1] claimed that phase studies of the antimony-oxygen system have often been complicated by the following factors (a) the oxides tend to exhibit allotropy; (b) both Sb(III) and Sb(V) ions can be present in oxides of different stoichiometries; and (c) the evolution of water from hydrated precursors does not necessarily yield the expected anhydrous oxides.

The research on Sb-O composition and structure by many researchers has been summarized. Antimony trioxide exists in two crystal structures, cubic and orthorhombic both of which are stable at room temperature [2, 3]. Cubic Sb_2O_3 , also known as senarmonite, has a structure based on Sb_4O_6 molecule [1, 4, 5]. This crystal was stable below 843 K [6] and can exist as molecules in the gas phase [2]. Meanwhile, orthorhombic Sb_2O_3 , also known as valentinite, has a layered structure, in which long chains (each “link” contains three O^{2-} ions and shares four Sb^{3+} ions) are held together by weak Sb-O interactions [5].



When heating senarmontite in the absence of oxygen, the first thermal effect to be observed is usually the onset of sublimation at ca. 775 K. Senarmontite is transformed to valentinite, at about 829 K with a melting point of 929 K [7, 8]. Finely ground valentinite has also been reported to oxidize at a lower temperature than senarmontite [2, 3]. In addition, Trofimov *et al.* [9] found that mixtures of senarmontite and valentinite do not oxidize additively. In their work, when finely divided senarmontite was oxidized in air, orthorhombic Sb_2O_4 also known as cervantite, was produced at 733 K. Under similar conditions, valentinite oxidized at 673 K. The oxidation of orthorhombic valentinite Sb_2O_3 to orthorhombic cervantite Sb_2O_4 as well as the reverse reduction is a topotactic reaction, where the structure of valentinite is completely preserved in cervantite.

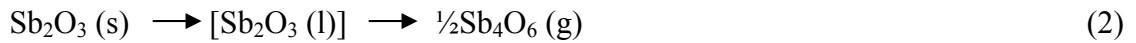
The oxidation involves very little change in the structure of valentinite, and the additional oxygen atoms in cervantite merely occupy positions along the empty channels present in the former. The mechanism has been proposed whereby the diffusion of oxygen atoms involving the making and breaking of bonds between (pentavalent) antimony and these oxygen atoms. The additional oxygen atoms in cervantite occupy positions along the empty channels available in the structure of valentinite and bridge the $(\text{Sb}_2\text{O}_3)_\infty$ chains in the direction a perpendicular to the length of the channels [10]. Molten Sb_2O_3 is very volatile between 925 and 1125 K, but it loses mass more slowly at higher temperatures [2, 3]. It seems probable that, on melting, valentinite forms a mobile liquid consisting of Sb_4O_6 molecules, which then associates to form polymeric Sb-O chains [2] and thus yields a much more viscous liquid phase. All the observations suggested that sublimation is critical in the oxidation of Sb_2O_3 [7].

In common with other elements in the B subgroups of the Periodic Table, antimony has a tendency to form mixed-valent compounds in which the two oxidation states may be represented by N and $N-2$ (where N is the principal state for the group) [1]. In Sb_2O_4 , the Sb(V) and Sb(III) ions are present in equal proportions [1, 11]. Therefore, the fact that some commercial samples are listed as “antimony(IV) oxide” can only be justified as a way of indicating the mean oxidation state of the metal ions, and so distinguishing the tetroxide from Sb_6O_{13} . There are two polymorphic forms of Sb_2O_4 *i. e.* orthorhombic α -phase (cervantite) and a high-temperature monoclinic β -phase [1]. According to Xiong *et al.* [12], pure α - Sb_2O_4 is inactive and inert.

Figure 1.1 (a) and (b) show a molecular structure of α - Sb_2O_4 and β - Sb_2O_4 . The α - Sb_2O_4 structure is similar to the β structure, but of a lower symmetry. A major difference between α and β forms is in the coordination of the Sb^{3+} ions. In the β structure four oxygen atoms are within bonding distance, whereas in α structure a fifth oxygen atom comes within bonding distance [13].

Between the two, the orthorhombic α -form (cervantite) [1, 14 and 15] is the more common; it is the usual product of the oxidation of Sb_2O_3 under air/oxygen, and of the decomposition of some of the higher oxides such as $\text{Sb}_2\text{O}_5 \cdot n\text{H}_2\text{O}$ [2] or Sb_6O_{13} [2, 16]. Cervantite is remarkably stable and is found not to undergo any physical or chemical change on heating below 1273 K, either in air or nitrogen [2, 3]. Above 1273 K, an endothermic process occurs [3], leading to a complete loss of mass. One possibility is that cervantite sublimates at high temperatures [2]. Accordingly, it has been proposed that

cervantite decomposes to yield oxygen and Sb_2O_3 , which immediately melts and volatilizes [3]:



Rogers and Skapski, quoted by Golunski [1], have suggested the following route for the transformation of $\alpha\text{-Sb}_2\text{O}_4$ to the monoclinic β -form:

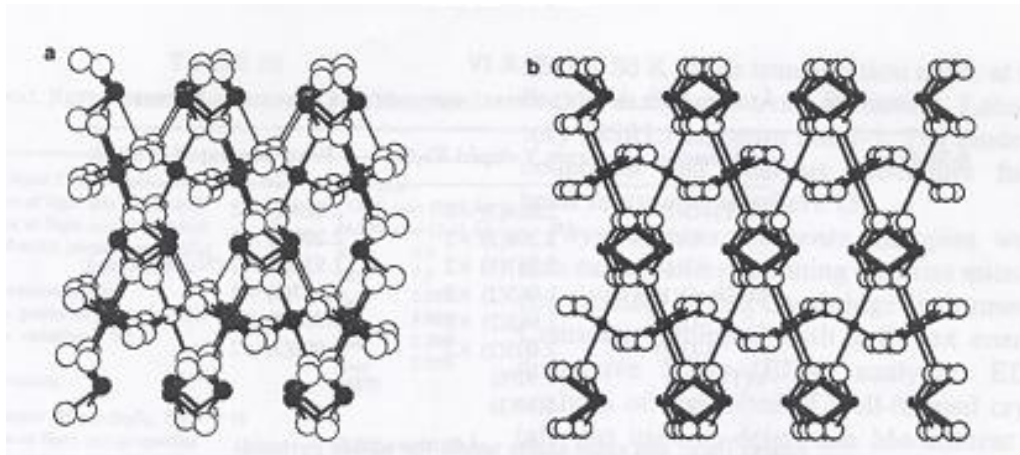
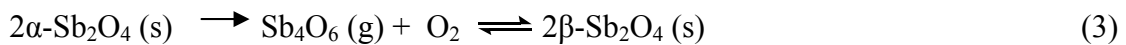
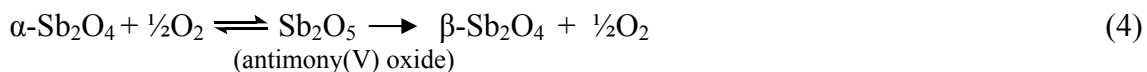


Figure 1.1: (a) α -antimony oxide ($\alpha\text{-Sb}_2\text{O}_4$). (b) β -antimony oxide ($\beta\text{-Sb}_2\text{O}_4$). Filled spheres represent Sb atoms; open spheres, oxygen atoms. Note the two kinds of coordination for the two types of Sb atoms. Sb^{5+} atoms are octahedrally coordinated. The asymmetric coordination of the Sb^{3+} is due to the presence of a lone electron pair; these form channels of electron density perpendicular to the views presented here. These Sb atoms are four-coordinate in the β form. In α form, fifth oxygen is weakly bonded to Sb^{3+} . There are two types of oxygen atoms in $\beta\text{-Sb}_2\text{O}_4$, one type bridges Sb^{5+} atoms only, while the second type bridges Sb^{3+} and Sb^{5+} atoms [13].

Under high pressure, the oxidation of the tetroxide [1] becomes more likely than its dissociation. Golunski *et al.* [1] suggested that the following sequence may, therefore apply:



The most common hydrated form of antimony(V) oxide (antimonic acid) has a pyrochlore-type structure [1, 17], in which anion vacancies may be occupied by oxygen atoms from the water molecules [1]. Olen'kova, quoted by Golunski, [1] also predicted that the maximum value of n should be 3 in $\text{Sb}_2\text{O}_5 \cdot n\text{H}_2\text{O}$, though this value is often exceeded. On heating $\text{Sb}_2\text{O}_5 \cdot n\text{H}_2\text{O}$ to 1273 K, most of the mass is lost below 1125 K [2]. The loss occurs in two stages where the first stage (350-475 K) is due to partial dehydration; while the second (925-1125 K) is the result of concurrent evolution of water of crystallization and of lattice oxygen, with the resultant formation of Sb_6O_{13} [2]. Cubic Sb_2O_5 loses oxygen progressively on heating above 673 K, leading eventually to the formation of orthorhombic Sb_2O_4 [3]. Anhydrous antimony(V) oxide cannot be prepared directly from $\text{Sb}_2\text{O}_5 \cdot n\text{H}_2\text{O}$ [1, 2].

The final antimony oxide that exists is Sb_6O_{13} which can be considered as intermediate phase between Sb_2O_5 and Sb_2O_3 in terms of both structure [1] and thermal stability [2]. There are several reasons why Sb_6O_{13} can be mistakenly identified as Sb_2O_5 , but it seems that the original cause was the widespread belief that Sb_2O_5 could be prepared by heating $\text{Sb}_2\text{O}_5 \cdot n\text{H}_2\text{O}$ until no further water was evolved.

1.2 Preparation of Antimony Oxide

1.2.1 Preparation Methods

The material properties are strongly affected by every step of the preparation together with the quality of the raw materials. The choice of a laboratory preparation of a given material depends on the physical and chemical characteristics desired in the final composition [18]. Nowadays, many methods and techniques have been discovered by researchers in order to synthesize the mono and mixed metal oxide systems with the best performance, which is very useful in industry.

Recently, however, to our knowledge, only a few studies on synthesis of the antimony oxide and its characteristics have been reported [19, 20]. This oxide can be readily synthesized with various well-developed techniques such as thermal vapor condensation [21, 22], hydrothermal method [20, 23] and sol-gel method [23, 24]. There are however some problems and limitations, such as complex technique, limited success with refractory metal for the gas condensation, high temperature and high pressure for the hydrothermal method [23]. Beside the weakness of the thermal vapor condensation, this method is considered to be the most appropriate for the production of nonagglomerated nanoparticles with clean surface [22]. The antimony trioxide was successfully synthesized under controlled atmosphere using the γ -ray radiation-oxidation route method or chemical method [19, 23]. Recently, scientists have developed a new method using the hybrid induction and laser heating (HILH) method. This method was claimed